



Universidad
Carlos III de Madrid



Peinado, C., Salvador, E. F., Alonso, A., Corrales, T., Baselga, J. & Catalina, F., (2002). Ultraviolet curing of acrylic systems: Real-time Fourier transform infrared, mechanical, and fluorescence studies. *Journal of Polymer Science, Part A: Polymer Chemistry*, 40 (23), pp. 4236–4244.

DOI: [10.1002/pola.10515](https://doi.org/10.1002/pola.10515)

© Wiley, 2002

Ultraviolet curing of acrylic systems: Real-time Fourier transform infrared, mechanical, and fluorescence studies

CARMEN PEINADO,¹ ENRIQUE F. SALVADOR,¹ ASUNCIÓN ALONSO,¹ TERESA CORRALES,¹ JUAN BASELGA,² FERNANDO CATALINA¹

¹Instituto de Ciencia y Tecnología de Polímeros, (CSIC), Juan de la Cierva ³, 28006 Madrid, Spain

²Universidad Carlos III de Madrid, Avda. Universidad 30, Leganes, 28911 Madrid, Spain

ABSTRACT

The photopolymerization of acrylic-based adhesives has been studied by Fourier transform infrared and fluorescence analysis in real time. Real-time infrared spectroscopy reveals the influence of the nature of the photoinitiator on the kinetics of the reaction. Furthermore, the incident light intensity dependence of the polymerization rate shows that primary radical termination is the predominant mechanism during the initial stages of the curing of the acrylic system with bis(2,4,6-trimethylbenzoyl) phenyl phosphine oxide (TMBAPO) as a photoinitiator. The fluorescence intensity of selected probes increases during the ultraviolet curing of the adhesive, sensing microenvironmental viscosity changes. Depending on the nature of the photoinitiator, different fluorescence–conversion curves are observed. For TMBAPO, the fluorescence increases more slowly during the initial stage because of the delay in the gel effect induced by primary radical termination. Mechanical tests have been carried out to determine the shear modulus over the course of the acrylic adhesive ultraviolet curing. In an attempt to extend the applications of the fluorescence probe method, we have undertaken comparisons between the fluorescence changes and shear modulus. Similar features in both curves confirm the feasibility of the fluorescence method for providing information about microstructural changes during network formation.

Keyword

Fuorescence monitoring
Ultraviolet curing
Infrared spectroscopy(FT-IR in realtime)
Kinetics (polym.)
Adhesives
Mechanical properties

INTRODUCTION

An adhesive is a complex mixture of substances that, when applied between two surfaces, provides material continuity for joining them and preventing their separation. In the last 50 years, the development of adhesives based on synthetic polymers has increased exponentially because of

the high-performance demand for technical applications. During the formation of an adhesive joint, two stages can be distinguished at least. First, the liquid formulation spreads over the substrates and, second, this formulation hardens to bear and transfer the loads that may appear during its in-service life. The first stage is controlled by the thermodynamics and kinetics of the wetting process, which depends on the physicochemical nature of both the substrates and the liquid formulation. The hardening stage is controlled by a wide variety of different chemical processes, but for high-performance adhesives, the polymeriza-

tion mechanism or curing is the preferred one. With regard to adhesive technology, the requirement for shortening curing times has brought a new approach to the use of formulations that will polymerize under ultraviolet (UV) or visible radiation. Photochemical polymerization has allowed the development of one-component adhesives that cure in a few minutes (or seconds) at room temperature. For the further development of adhesive technology, a knowledge of the polymerization processes is of great interest because the final (mechanical) properties of these materials are mainly related to the extent of cure along with the nature of the binder.

The online monitoring of polymerization reactions requires a determination of the degree of conversion in real time. Different techniques have been used in the past, such as differential scanning calorimetry and Fourier transform infrared (FTIR), which are based on the measurement of different macroscopic magnitudes. The fluorescence probe method¹⁻⁷ has been shown to be very useful for following photopolymerization because the emission changes are related to the mutual rearrangements occurring in the microenvironment of the probe, more particularly, sensing the increase in rigidity during polymerization. Therefore, a nonlinear correlation should be expected between the fluorescence and the degree of conversion when the whole process is studied. Furthermore, fluorescence has found numerous applications in polymer science.⁸⁻¹⁰ Some examples include studies of (1) the molecular structure, first- and second-order transitions (the glass-transition, γ -transition, and β -transition temperatures), end-to-end distances, and crystallinity; (2) associations and aggregations in water solutions of polyelectrolytes and amphiphilic polymers; (3) polycomplex formation; (4) the miscibility of polymer blends and interpenetration of polymers; (5) the microheterogeneity of polymer solutions; (6) conformational transitions in solution, including local and segmental displacements; (7) energy transfer, including the antenna effect; (8) orientation and residual stresses; and (9) sol-gel transitions. The versatility of this technique shows that fluorescence-based methods will allow us to gain a deeper insight into several processes, including photopolymerization.

The monitoring of polymerization has also been carried out by means of rheometry and dynamomechanical analysis.^{11,12} However, few efforts have been devoted to studying the mechanical

properties over the course of curing. Recently, Smirnov et al.¹³ pointed out the internal stresses and shrinkage defects on the network formation process influencing the strength properties of adhesive bonds as well as the nature of its failure.

The aim of this work is to find a correlation between fluorescence and conversion during the UV curing of an acrylic adhesive with two different photoinitiators. Real-time FTIR has been used to measure the acrylate double-bond conversion at different irradiation times, and the changes in the fluorescence intensity have been measured in real time. Furthermore, we have attempted to correlate our results with mechanical tests. In this regard, the shear moduli of the adhesive joints have been measured during UV curing.

EXPERIMENTAL

Fluorescent Probes and Acrylic Adhesives

4-Dimethylamino-4'-nitrostilbene (DMANS), 2-hydroxy-4-dimethylamino-4'-nitrostilbene (2OHDEANS), and 4-dimethylaminophenyl-4'-nitrophenylbutadiene (DMANBu) were synthesized to be used as fluorescent probes as previously described.¹⁴ The synthesis of 4-(*N,N'*-diethyl)amino-7-nitrobenz-2-oxa-1,3-diazole (NBD-NEt₂) and a methacrylic derivative (NBD-NAcr) have been earlier described.¹⁵ Molecular formulas of stilbene derivatives and the NBD fluorescent probes are shown in Figure 1.

The adhesive formulation L312 was provided by Loctite España. The fractionation and analysis of the components of L312 give the following composition. This adhesive comprises a mixture of 50% polyurethane-methacrylate resin, 35-40% hydroxyalkyl methacrylate, 5-10% acrylic acid, 1-3% cumene hydroperoxide, 0.1-1% tributylamine, and 0.1-1% trimethoxy[3-(oxiranylmethoxy)propyl]silane as an adhesion promoter.

The commercial photoinitiators 2-benzyl-2-*N,N*-dimethylamino-1-(4-morpholinophenyl)-1-butanone (DBMP; Irgacure 369) and bis(2,4,6-trimethylbenzoyl) phenyl phosphine oxide (TMBAPO; Irgacure 819) were provided by Ciba Specialty Chemicals. The mechanisms of fragmentation of both photoinitiators under UV-light exposure are shown in Scheme 1.

Sample Preparation

The fluorescent probe (ca. 0.03% w/w) and the photoinitiator (1% w/w) were dissolved in the ad-

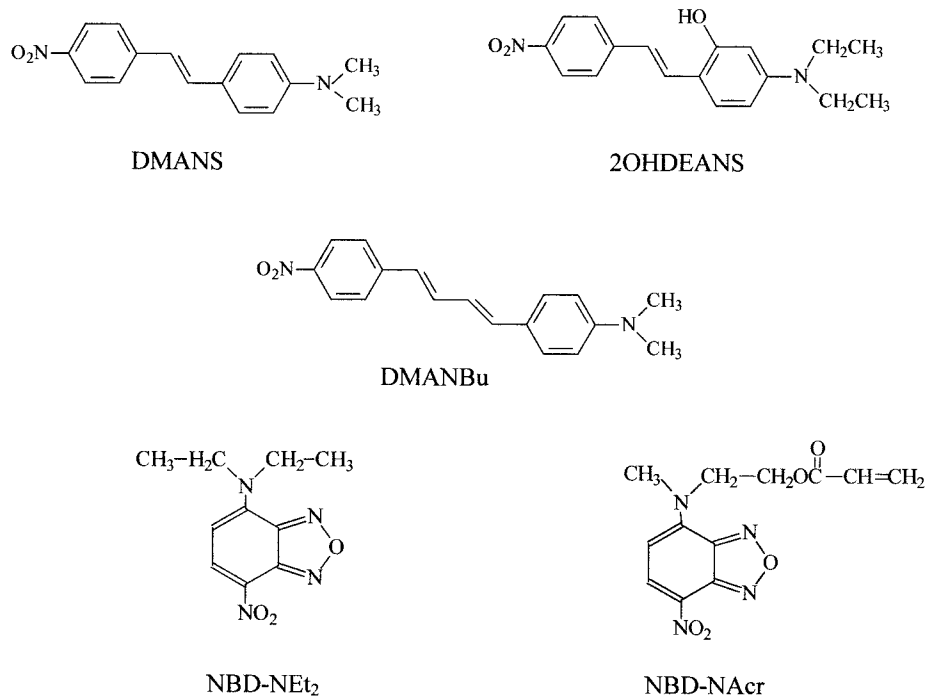
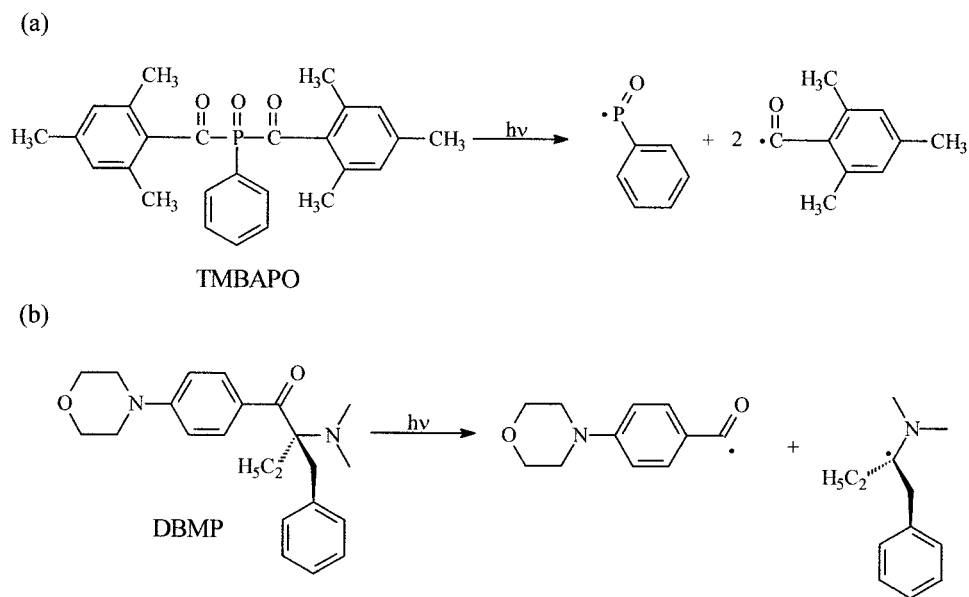


Figure 1. Chemical structures and abbreviations of the fluorescent probes used in this work.

hesive formulation. The photocurable formulations were applied as a uniform layer coating on a polyethylene film or aluminum foil and then were

covered with a low-density polyethylene (LDPE) film (40 μm thick) that did not absorb at the infrared (IR) frequencies selected to follow the



Scheme 1. Photofragmentation mechanisms of the photoinitiators DBMP and TMBAPO under UV irradiation.

photopolymerization reaction nor at the excitation/emission and UV-irradiation wavelengths. The function of the LDPE film was to prevent oxygen diffusion from the atmosphere into the sample during the irradiation at room temperature. The photosensitive coatings (15 μm) were obtained by controlled pressing.

Both photoinitiators also absorb excitation light (355 nm); however, fluorescence from the photoinitiator does not interfere the fluorescence spectra of the probe because of their low fluorescence quantum yield.

Monitoring the UV Curing of Acrylic Systems

The UV curing of the adhesive formulations was carried out by irradiation with a 400-W mercury lamp (Macam-Flexicure irradiation system) at room temperature under an air atmosphere until limiting conversion. The incident intensity was measured with a Scientech H310D photocalorimeter and was varied with different interference filters in front of the sample. For all samples, the disappearance of double bonds and the fluorescence changes of the probes were monitored by FTIR and luminescence spectroscopy, both under real-time conditions. Experimental details have been described previously.¹⁶

FTIR in Real Time

Real-time infrared (RTIR) measurements were carried out in a Nicolet 520 IR spectrophotometer provided with a Fourier transform algorithm. The samples were placed over a specular reflection accessory in the IR spectrophotometer, in which they were simultaneously exposed to the UV light and to the IR analyzing beam. The decrease in the absorbance at 817 cm^{-1} (corresponding to the disappearance of the acrylate double bond) was annualized by means of a software program to record data in real time (acquisition time = 0.3 s).

Fluorescence Spectroscopy in Real Time

The fluorescence emission was collected with a monochromator (Oriel MS257) during UV irradiation of the acrylic adhesives. The spectra were recorded with an intensified charge coupling device (CCD) camera (Andor ICCD-408) with a camera exposure time of 1 μs . The excitation wavelength was fixed at 355 nm from the Nd-YAG laser (Quanta-Ray, Spectra Physics). It was checked that the excitation laser beam used for

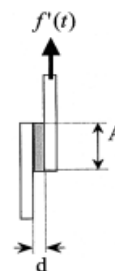


Figure 2. Geometrical disposition of the specimens for mechanical tests.

analysis did not contribute to polymerization initiation, and for this purpose, an attenuator was placed in front of the sample to diminish the incident light.

Mechanical Properties

An MTS Synergie 200 (100N) computer-aided dynamometer was used for measuring the shear strength of overlapped adhesive joints. The following conditions were fixed: a deformation rate of 0.5 mm/min and a maximum load of 100 N.

The adhesive was dispensed onto two glass slides (60 mm \times 25 mm \times 5 mm) previously rinsed with isopropanol and air-dried. Joints were then assembled immediately, and any excess exuded adhesive was removed from joint edges by tissue wiping to avoid fillet formation. The thickness of the adhesive layer was carefully controlled to be 15 μm . The specimens depicted in Figure 2 are well suited for testing joints. The test pieces were placed between the clamps of the dynamometer and then irradiated with a medium-pressure Hg lamp at different curing times. After the specimen was mounted in the fixture of the testing machine, the end of the specimen was supported to keep the beam orthogonal to the direction of the applied load. After the light was switched off, the tests were performed under normal conditions in agreement with ASTM Standard 1002-64. The shear modulus (G) was determined from the slope of the initial linear portion of the stress-strain plots:

$$G = \frac{F/A}{l/d} \quad (1)$$

where F is the load (N), l is the displacement between clamps (m), A is the area of the overlapped joint, and d is the thickness of the adhe-

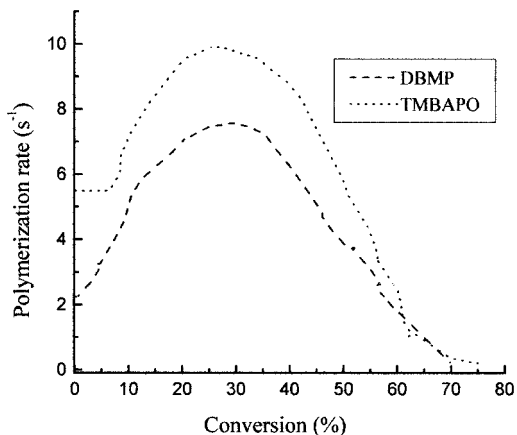


Figure 3. Plot of the polymerization rate as a function of conversion for the UV curing of L312 with the two photoinitiators DBMP and TMBAPO. $I_0 = 1.84 \text{ mW} \cdot \text{cm}^{-2}$.

sive layer. The average value was determined from the data of three tested specimens.

RESULTS AND DISCUSSION

The polymerization rate, fluorescence intensity changes, and shear modulus have been *in situ* monitored over the course of the UV curing of the acrylic commercial adhesive L312 with different photoinitiators, DBMP and TMBAPO.

Kinetic Study by RTIR

First, the reactions between the photoinitiator and fluorescent compound were examined. No reaction was observed, and this indicated that they should not modify the properties of the final material. Therefore, the kinetic profiles measured by FTIR in real time are the same in the absence and presence of the fluorescent probes. Figure 3 plots the polymerization rate versus conversion. The initial polymerization rate for TMBAPO is higher than that for DBMP. The irradiation of the TMBAPO photoinitiator gives rise to phosphonyl radicals, which are more reactive than the carbon-centered radicals, photogenerated by the photolysis of DBMP (Scheme 1). Therefore, higher polymerization rates are achieved with the acyl phosphide photoinitiator.

As expected for diffusion-controlled kinetics, a dramatic increase in the polymerization rate is observed at low conversions (ca. 6% for TM-

BAPO). This autoacceleration effect is due to the decreased mobility of the growing macroradicals as the viscosity increases, which causes a reduction in the termination rate constant, and as a result, the macroradical concentration increases (and, therefore, so does the polymerization rate).

The magnitude and onset of the gel effect have been shown to depend strongly on the monomer structure for various multifunctional (meth)acrylates. Goodner and Bowman¹⁷ studied the influence of primary radical termination on the gel effect, showing that as the primary radical termination rate constant increases, the autoacceleration rate is diminished. Furthermore, the increase in the primary radical concentration (e.g., increasing irradiation light intensities) drives the primary radical termination to compete with bimolecular termination, becoming the dominant mechanism earlier in the reaction under certain conditions.

During the UV curing of L312 with two different photoinitiators, a certain reduction of the gel effect is observed when TMBAPO is compared to DBMP (Fig. 3). This behavior indicates that primary radical termination plays a role with the acyl phosphide photoinitiator and would reduce the kinetic chain length and, therefore, the molecular weight. Furthermore, at a 30% conversion, the polymerization rate is reduced because of a decrease in the propagation rate constant associated with the low diffusivity of the monomer into the polymer matrix.

The influence of the incident light intensity on the polymerization rate was determined to investigate the mechanism of the termination reactions. Plots of conversion versus irradiation time during the UV curing of L312 under different irradiation conditions are shown in Figure 4 with DBMP and TMBAPO as photoinitiators. The reaction rate is proportional to the intensity of the incident light (I_0), and the final conversion (0.75) is independent of the light intensity with TMBAPO. However, the limiting conversion increases at a high value of I_0 in comparison with those measured at low intensities (from 0.67 at 0.24 mW/cm^2 to 0.85 at 1.84 mW/cm^2) when DBMP is used as a photoinitiator.

The dependence of the rate of polymerization (R_p) on the light intensity under steady-state conditions is expressed by eq 2:

$$R_p = -d[M]/dt = k(x) \cdot [M]^\alpha I_0^\beta \quad (2)$$

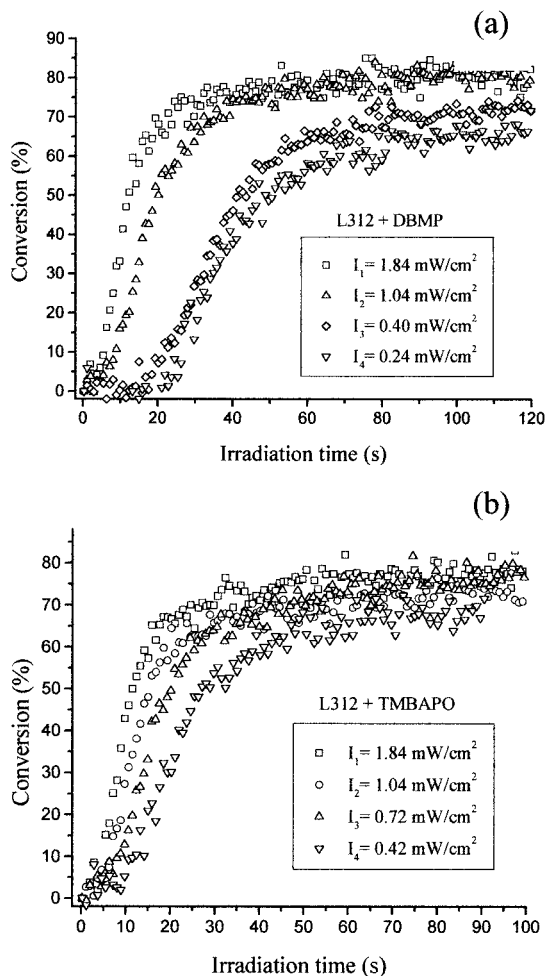


Figure 4. Time dependence of the double-bond conversion for the UV curing of L312 initiated by various light intensities with the photoinitiators (a) DBMP and (b) TBAPO.

where $[M]$ is the concentration of acrylate double bonds, t is the time, and $k(x)$ is a quantity depending on the conversion x . The exponents α and β are related to the mechanism of network formation. It is well known¹⁸ that β depends on the kind of termination; that is, $\beta = 1$ means first-order termination, $\beta = 0.5$ means bimolecular termination, $\beta < 0.5$ means primary radical termination, and $0.5 < \beta < 1$ means combined first- and second-order termination. The method for the determination of β from eq 3 has been previously described:¹⁹

$$-\ln x = k'(x) \cdot I_0^\beta \cdot t' \quad (3)$$

The time t , which is necessary to obtain a conversion at light intensity I , must be determined from

Figure 4 to estimate β . This complicated procedure is necessary because in viscous media the reaction constant k is a function of conversion, and so the kinetics must be related for one specific conversion. The slope of the double logarithmic plot of the irradiation time versus the light intensity yields the value of β at a specific conversion degree:

$$\ln \frac{[-\ln(1-x)]}{t} = \ln(k) + \beta \ln(I) \quad (4)$$

Table 1 summarizes the β values for different photoinitiators at various degrees of conversions. The value of β varies with the nature of the photoinitiator. For DBMP, the value of $\beta = 0.5$ – 0.6 indicates a predominant second-order termination reaction. A value of $\beta < 0.5$ with TBAPO confirms a primary radical termination mechanism combined with polymer radical recombination, as we pointed out previously.

Fluorescence Monitoring

The photocuring of L312, with TBAPO and DBMP as photoinitiators, was followed by FTIR and fluorescence in real time. Figure 5 shows the plot of the fluorescence integrated intensity as a function of the acrylate double-bond conversion with two families of fluorescent probes: stilbene derivatives and NBD probes.

DMANS shows the highest sensitivity, whereas the NBD derivatives (NBD-NEt₂ and NBD-NAc) show a slightly lower sensitivity, as does DMANBu. Moreover, the fluorescence changes during the whole process, especially during the last stage, and this is more interesting from an applied viewpoint. Surprisingly, the curves show different profiles depending on the photoinitiator used for the UV curing of L312. In this sense, it is interesting to compare fluorescence curves during the photopo-

Table 1. Values of the Exponent β for the Photoinitiators DBMP and TBAPO during the UV Curing of the Adhesive Formulation L312

Conversion (%)	TBAPO β	DBMP
0.15	0.33	0.64
0.20	0.30	0.52
0.25	0.39	0.53
0.30	0.36	0.56

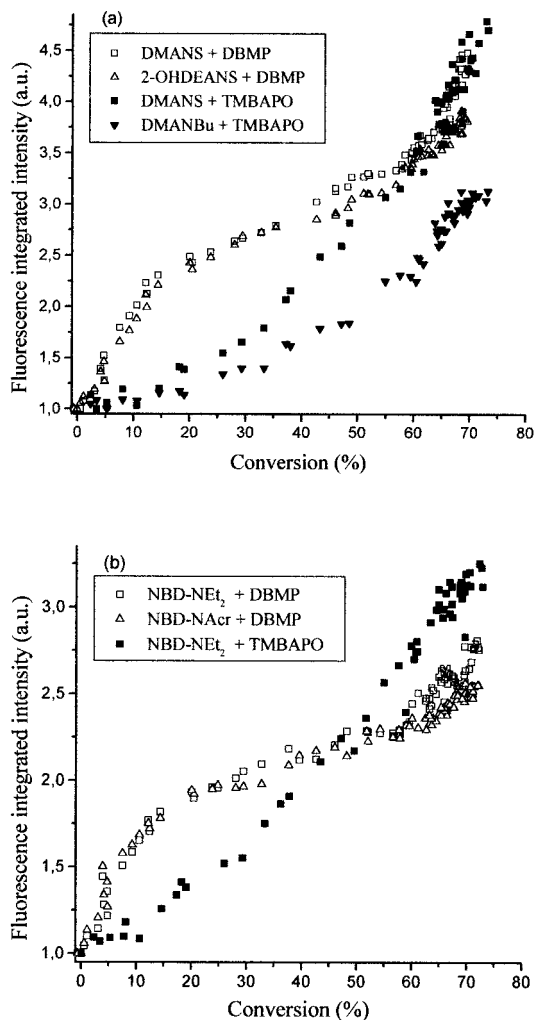


Figure 5. Plots of the fluorescence versus the conversion of the UV curing of the adhesive L312 with DBMP and TMBAPO as photoinitiators. The fluorescent probes were (a) DMANS, DMANBu, and 2OHDEANS and (b) NBD derivatives. $I_0 = 1.84 \text{ mW} \cdot \text{cm}^{-2}$.

polymerizations of L312 with DBMP and of L312 with TMBAPO. During the network formation with DBMP, higher fluorescence changes are measured at the first stage of conversion (up to approximately 15%), whereas further progress of the reaction modifies more slowly the fluorescence parameters. However, when TMBAPO is used as a photoinitiator, small variations of the fluorescence intensity are observed up to 20–30% conversion, and then the fluorescence intensity increases sharply with conversion. Fluorescence changes are induced by variations in the viscosity and polarity in the microenvironment of the probe. Therefore, this feature indicates that the

local rigidity of the probe microenvironment increases more rapidly in L312 with DBMP than in L312 with TMBAPO. This effect is an indication of microstructural changes during the network photogeneration, induced with different photoinitiators. Furthermore, this proposal agrees with FTIR results, which show that the kinetics of the curing reaction are influenced by the nature of the photoinitiator. During the initial stages of UV curing of L312 with TMBAPO, primary radical termination plays an important role. As a result of this termination mechanism, the kinetic chain length diminishes, and so does the molecular weight; this brings a delay of the gel effect. This behavior can explain why the fluorescence increases more slowly during the initial stages of curing with TMBAPO.

Mechanical Measurements

Figure 6 gives kinetic curves of the change in the shear modulus over the course of the UV curing of the acrylic adhesive L312 with different photoinitiators. A rapid increase in the value of the modulus can be seen with DBMP. However, the shear modulus of the adhesive formulation containing TMBAPO shows an inhibition time before its value increases as the polymerization progresses. This feature has been correlated with the delay of the autoacceleration effect. Because the composition formulation only changes the photoinitiator, the delay of the gel effect with TMBAPO has been

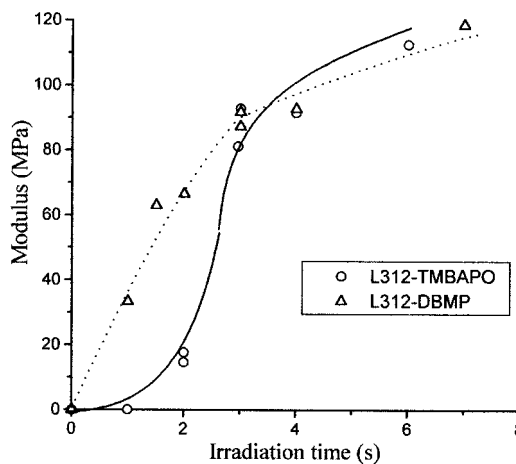


Figure 6. Time dependence of the shear modulus during joint adhesive L312 formation with DBMP and TMBAPO as photoinitiators. $I_0 = 1.84 \text{ mW} \cdot \text{cm}^{-2}$.

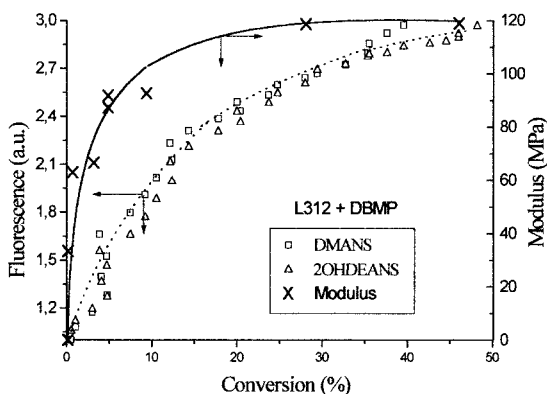


Figure 7. Plot of the fluorescence changes versus the conversion during the UV curing of L312 with DBMP. The fluorescent probes were DMANS and 2OHDEANS. On the right axis, the shear modulus of the adhesives formulations as a function of conversion is plotted. $I_0 = 1.84 \text{ mW} \cdot \text{cm}^{-2}$.

attributed to a decrease in the primary chain length due to the primary radical termination.

The shear modulus is a measurement of the stiffness of the material and increases from a soft material to a hard material. From a macroscopic point of view, photocuring can be considered, therefore, a hardening of a material. Moreover, fluorescent probes are sensitive to changes in the local rigidity of the medium. In a medium in which molecular mobility is restricted, the fluorescence emission increases because of the associated restriction in the nonradiative relaxation pathway of the excited state of the probe. This nonradiative process normally involves some kind of vibrational coupling between the excited state and the environment, which behaves as a thermal bath. For these reasons, a correlation should be found between fluorescence and modulus during a cure process.

Figure 7 shows a comparison of fluorescence and shear modulus changes during the UV curing of the acrylic adhesive L312 with DBMP as a photoinitiator. The fluorescence increase follows the same trend as that for the modulus changes with conversion. As a result of the crosslinking, the rigidity of the material increases, as does the fluorescence emission, because the nonradiative relaxation pathway is significantly restrained. A similar behavior is observed for the system L312 and TMBAPO. A comparison between Figures 5 and 6 shows that, in this case, both fluorescence and shear modulus increase after an inhibition time (not observed with DBMP). These new re-

sults corroborate our proposal that the fluorescence method can be useful for the analysis of microstructural changes during UV curing.

CONCLUSIONS

The combination of RTIR, mechanical tests, and fluorescence experimental data have allowed us to clarify the influence of the photoinitiator nature on the UV curing of an acrylic-based adhesive. The high reactivity of phosphonyl oxide primary radicals photogenerated from TMBAPO results in a primary radical termination mechanism. As a result of this predominant termination mechanism, the primary kinetic chain length is shortened, the molecular weight is reduced, and the gel effect is diminished.

For first time, the fluorescence has been correlated with microstructural changes occurring over the course of polymerization. Therefore, the fluorescence method is presented here as a powerful tool for studying deep photopolymerization reactions because it can provide information about the process in a more sophisticated fashion than a simply correlation of the fluorescence extent of cure.

The authors thank the Union European Commission for funding through the BRITE-Euram Project (BE97-4472). Gratitude is also extended to Plan Nacional I+D+I (Ministerio de Ciencia y Tecnología) for its financial support (MAT2000-1671) and to Comunidad Autónoma de Madrid (07N/0002/1998). The authors thank K. Dietliker (Ciba Specialty Chemicals) for providing the photoinitiators and Loctite España for providing the adhesives.

REFERENCES AND NOTES

1. Jager, W. F.; Volkers, A. A.; Neckers, D. C. *Macromolecules* 1995, 28, 8153.
2. Wang, Z. J.; Song, J. C.; Bao, R.; Neckers, D. C. *J Polym Sci Part B: Polym Phys* 1996, 34, 325.
3. Yu, J. W.; Sung, C. S. P. *J Appl Polym Sci* 1997, 63, 1769.
4. Strehmel, B.; Malpert, J. H.; Sarker, A. M.; Neckers, D. C. *Macromolecules* 1999, 32, 7476.
5. Jager, W. F.; Lungu, A.; Chen, D. Y.; Neckers, D. C. *Macromolecules* 1997, 30, 780.
6. Serrano, B.; González-Benito, J.; Cabanelas, J. C.; Bravo, J.; Baselga, J. *J Fluoresc* 1997, 7, 341.

7. Bosch, P.; Fernández-Arizpe, A.; Catalina, F.; Mateo, J. L.; Peinado, C. *Macromol Chem Phys* 2002, 203, 336–345.
8. Rabek, J. F. *Mechanism of Photophysical Processes and Photochemical Reactions in Polymers*; Wiley: Chichester, England, 1987.
9. Itagaki, H. In *Experimental Methods in Polymer Science*; Tanaka, T., Ed.; Academic: New York, 2000; pp 155–254.
10. Huang, H. W.; Horie, K. *Trends Polym Sci* 1997, 5, 407.
11. Kim, D. S.; García, M. A.; Macosko, C. W. *Int Polym J* 1998, 13, 162.
12. Lee, D. S.; Han, C. D. *Polym Eng Sci* 1987, 27, 955.
13. Smirnov, Y. N.; Golodkva, F. M.; Korotkov, V. N. *Int Polym Sci Technol* 2000, 27, 46.
14. Peinado, C.; Salvador, E. F.; Catalina, F.; Lozano, A. E. *Polymer* 2001, 42, 2815–2825.
15. Alonso, A.; Catalina, F.; Salvador, E. F.; Peinado, C. *Macromol Chem Phys* 2001, 202, 2293.
16. Peinado, C.; Salvador, E. F.; Baselga, J.; Catalina, F. *Macromol Chem Phys* 2001, 202, 1924–1934.
17. Goodner, M. D.; Bowman, C. *Macromolecules* 1999, 32, 6652.
18. Bajdala, J.; Müller, U.; Wartewig, S.; Winkler, K. *Makromol Chem* 1993, 194, 3093.
19. Timpe, H. J.; Strehmel, B.; Roch, F. H.; Fritzsche, K. *Acta Polym* 1987, 38, 238.